

# Temperature gradient driven lasing and stimulated cooling

K. Sandner and H. Ritsch

*Institute for Theoretical Physics, Universität Innsbruck, Technikerstrasse 25, 6020 Innsbruck, Austria*

(Dated: June 14, 2021)

A laser can be understood as thermodynamic engine converting heat to a coherent single mode field close to Carnot efficiency. From this perspective spectral shaping of the excitation light generates a higher effective temperature on the pump than on the gain transition. Here, using a toy model of a quantum well structure with two suitably designed tunnel-coupled wells kept at different temperature, we study a laser operated on an actual spatial temperature gradient between pump and gain region. We predict gain and narrow band laser emission for a sufficient temperature gradient and resonator quality. Lasing appears concurrent with amplified heat flow and points to a new form of stimulated solid state cooling. Such a mechanism could raise the operating temperature limit of quantum cascade lasers by substituting phonon emission driven injection, which generates intrinsic heat, by an extended model with phonon absorption steps.

PACS numbers: 42.50.Pq

Lasing is facilitated by implementing gain within an optical resonator. For stimulated emission based amplification this requires an inverted population distribution between the amplifier quantum states [1]. In theoretical descriptions pumping to generate inversion can be well described by coupling reservoirs of different temperature to the pump, the injection and the lasing transition [2, 3]. Practically this requires precise spectral design of the pump radiation to overlap mainly with the pump transition with strong suppression on the lasing and injection transitions to yield inversion. Interestingly, such inversion can be consistently mimicked by simply assuming an effective negative temperature on the lasing transition [4]. At optical frequencies almost no thermal photons are present at room temperature and simple filtering of the pump light is sufficient. However, simple spectral shaping in the far infrared or even THz regime is practically hampered by ubiquitous thermal quanta, which create strong restrictions on the laser operating temperature [5].

In this paper we study possibilities to directly use spatial temperature gradients instead of spectral pump design to generate inversion and facilitate gain and lasing. Although we mostly concentrate on the basic principles and mechanisms of such a setup, we also try to connect to a possible real world implementation based on designed quantum well structures. Here the optical properties and level structures in far infrared or even THz regime can be precisely engineered. While such a temperature gradient laser at first seems more of conceptual than of practical importance, the underlying principle can be easily generalized to a system with different pump steps. In particular thermal or phonon absorption based injection steps to the gain transition lead to interesting modification of the thermal operation conditions of such a laser. Lasing can be tied to thermal absorption and heat flow to avoid unwanted heating and control heat flow [6].

The model we study is a simple structure comprised

of two quantum wells coupled to a cavity. A sketch is shown in Fig. 1. The Hamiltonian describing a system of  $N$  two-well structures coupled to a single cavity mode is given by  $H = H_0 + H_I$  with

$$H_0 = \hbar\omega_m a^\dagger a + \hbar \sum_{j=1}^N \left[ \omega_u |u_j\rangle \langle u_j| + \omega_l |l_j\rangle \langle l_j| + \sum_{k=1}^4 \omega_{I_k} |I_{k,j}\rangle \langle I_{k,j}| \right] \quad (1)$$

and the interaction Hamiltonian

$$H_I = \hbar g \sum_{j=1}^N (a |u_j\rangle \langle l_j| + a^\dagger |l_j\rangle \langle u_j|) + \hbar \sum_{j=1}^N (J_1 |I_{4,j}\rangle \langle I_{3,j}| + J_2 |I_{2,j}\rangle \langle I_{1,j}| + h.c.) \quad (2)$$

The energy eigenstates are denoted by  $|I_{1,j}\rangle, \dots, |I_{4,j}\rangle, |u_j\rangle$  and  $|l_j\rangle$  with the eigenenergies  $\hbar\omega_{I_1}, \dots, \hbar\omega_{I_4}, \hbar\omega_u$  and  $\hbar\omega_l$  and  $a^\dagger$  is the creation operator for a photon in the cavity mode with frequency  $\omega_m$ . The coupling between the  $u \rightarrow l$  transition and the mode is described by the coupling rate  $g$ . Tunneling between the states  $|I_{1,j}\rangle$  and  $|I_{2,j}\rangle$  and the states  $|I_{3,j}\rangle$  and  $|I_{4,j}\rangle$  is controlled by the tunneling matrix elements  $J_1$  and  $J_2$ . For the forthcoming analysis we define all frequencies with respect to  $\omega_l$  and switch to a frame rotating with  $\omega_m$  introducing the detuning  $\Delta_u = \omega_u - \omega_m$ . The dynamics of the reduced density matrix is described by the master equation

$$\frac{d}{dt}\rho = \frac{i}{\hbar} [\rho, H] + \mathcal{L}[\rho] \quad (3)$$

where the Liouvillian  $\mathcal{L}$  describes dissipative processes, including the coupling to the environment at finite temperature, see supplementary material.

The decay rate of the cavity is denoted by  $\kappa$ , while the spontaneous emission rates of the remaining transitions

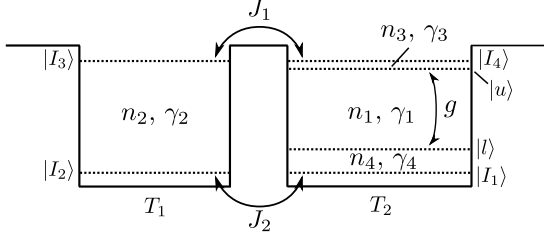


FIG. 1. Sketch of the two-well structure and the energy levels. The wave functions are assumed to be well localized in each well while the coupling is described by the tunneling constants  $J_1$  and  $J_2$ .

are denoted by  $\gamma_1, \dots, \gamma_4$ . The thermal photon number at the transition frequencies  $\omega_1 = \omega_u - \omega_l$ ,  $\omega_2 = \omega_{I_3} - \omega_{I_2}$ ,  $\omega_3 = \omega_{I_4} - \omega_u$  and  $\omega_4 = \omega_l - \omega_{I_1}$  at temperature  $T$  is denoted by  $n_i(T)$  ( $i = 1, \dots, 4$ ).

We assume that we have a temperature gradient across a sample containing  $N$  two-well structures and that  $T_1 > T_2$  in each structure. As  $T_1 \neq 0$  we will find population in the state  $|I_3\rangle$ . Via the tunnel-coupling  $J_1$  the state  $|I_2\rangle$  gets populated as well. Due to the lower temperature  $T_2$  of the second well the population is preferably transferred to the state  $|u\rangle$ . With a certain probability a photon is created in the cavity and leaves it. The cycle ends with the tunneling from state  $|I_1\rangle$  to  $|I_2\rangle$ .

Using Eq. (3) we calculate operator expectation value equations for the populations in each state and the quantities they couple to [7]. The equations are truncated to include only second order correlation functions. The population of the state  $|u_j\rangle$  is described by

$$\begin{aligned} \frac{d}{dt} \langle |u_j\rangle \langle u_j| \rangle &= -ig (\langle a |u_j\rangle \langle l_j| \rangle - \langle a^\dagger |l_j\rangle \langle u_j| \rangle) \\ &\quad - (2\gamma_1 (n_1 + 1) + 2\gamma_3 n_3) \langle |u_j\rangle \langle u_j| \rangle \\ &\quad + 2\gamma_1 n_1 \langle |l_j\rangle \langle l_j| \rangle \\ &\quad + 2\gamma_3 (n_3 + 1) \langle |I_{4,j}\rangle \langle I_{4,j}| \rangle, \end{aligned} \quad (4)$$

where we omitted the temperature dependence of the  $n_i$  and used the assumption of total phase invariance ( $\langle a \rangle = \langle |u_j\rangle \langle l_j| \rangle = 0$ ) to simplify the expansion of third order expectation values [8]. This leads to the next equation

$$\begin{aligned} \frac{d}{dt} \langle a |u_j\rangle \langle l_j| \rangle &= i\Delta_u \langle a |u_j\rangle \langle l_j| \rangle \\ &\quad - ig ([1 + \langle a^\dagger a \rangle] \langle |u_j\rangle \langle u_j| \rangle - \langle a^\dagger a \rangle \langle |l_j\rangle \langle l_j| \rangle) \\ &\quad - (\kappa + \gamma_1 (2n_1 + 1) + \gamma_3 n_3 + \gamma_4 (n_4 + 1)) \langle a |u_j\rangle \langle l_j| \rangle \\ &\quad - ig (N - 1) \langle |l_j\rangle \langle u_j| |u_k\rangle \langle l_k| \rangle \end{aligned} \quad (5)$$

which describes the rate at which excitations are transferred between the cavity and the structure. The number of photons follows  $\frac{d}{dt} \langle a^\dagger a \rangle = -2\kappa \langle a^\dagger a \rangle + 2\kappa n_1 - igN (\langle a^\dagger |l_j\rangle \langle u_j| \rangle - \langle a |u_j\rangle \langle l_j| \rangle)$ . In the last line of Eq. (5) we see that cooperative effects between the structures emerge as a result of the common interaction with

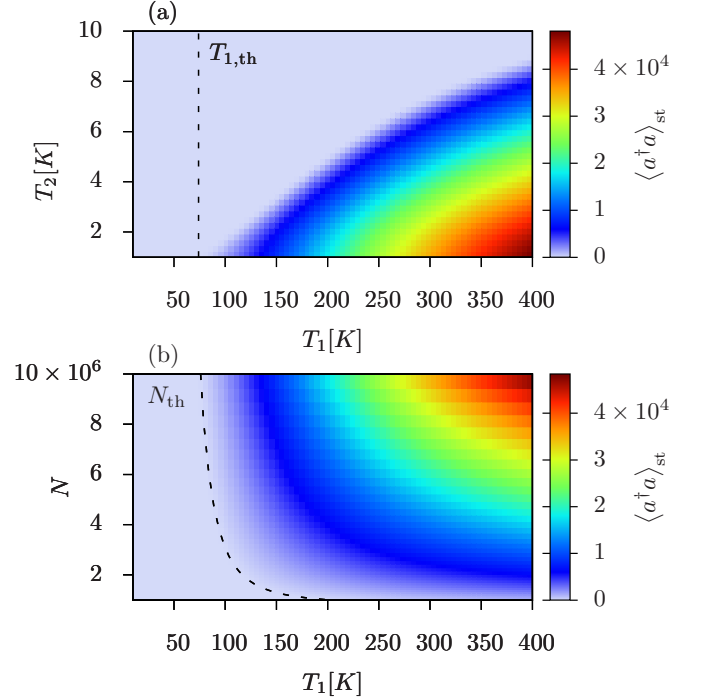


FIG. 2. (Color online) (a) Numerical solution for the steady state number of photons  $\langle a^\dagger a \rangle_{st}$  in the cavity as a function of  $T_1$  and  $T_2$ . The number of structures was chosen to be  $N = 10^7$ . The dashed line indicates  $T_{1,th}$  necessary to obtain cooperative behavior (valid for  $T_2$  small enough to justify setting  $n_1 = n_3 = n_4 = 0$ ). (b)  $\langle a^\dagger a \rangle_{st}$  as a function of  $T_1$  and  $N$  ( $T_2 = 0.1$  K). The analytical solution gives  $N_{th}(T_1)$  (dashed line) and reliably predicts the onset of cooperative behavior and hence a significant increase in  $\langle a^\dagger a \rangle_{st}$ .

the cavity. We find

$$\begin{aligned} \frac{d}{dt} \langle |l_j\rangle \langle u_j| |u_k\rangle \langle l_k| \rangle &= -ig [(\langle a^\dagger |l_j\rangle \langle u_j| \rangle - \langle a |u_j\rangle \langle l_j| \rangle) \\ &\quad \times (\langle |u_j\rangle \langle u_j| \rangle - \langle |l_j\rangle \langle l_j| \rangle)] \\ &\quad - (2\gamma_1 (2n_1 + 1) + 2\gamma_3 n_3 + 2\gamma_4 (n_4 + 1)) \\ &\quad \times \langle |l_j\rangle \langle u_j| |u_k\rangle \langle l_k| \rangle. \end{aligned} \quad (6)$$

In addition we calculate equations for  $\langle |l_j\rangle \langle l_j| \rangle$ ,  $\langle |I_{i,j}\rangle \langle I_{i,j}| \rangle$  ( $i = 1, 2, 3, 4$ ),  $\langle |I_{1,j}\rangle \langle I_{2,j}| \rangle$  and  $\langle |I_{3,j}\rangle \langle I_{4,j}| \rangle$ .

Approximate analytical solutions can be deduced under certain assumptions and give insight into the main mechanisms [9]. We assume that  $T_2$  is small enough to justify setting  $n_1 = n_3 = n_4 = 0$  and that  $\Delta_u = 0$ . By keeping only the decay term proportional to  $\kappa$  and the last line in Eq. (5), where we approximate  $N - 1 \approx N$ , we obtain the steady-state

$$\langle a |u_j\rangle \langle l_j| \rangle_{st} = -\frac{igN}{\kappa} \langle |l_j\rangle \langle u_j| |u_k\rangle \langle l_k| \rangle_{st}. \quad (7)$$

Under the assumption of negligible  $T_2$  and by using Eq. (7) it is possible to calculate approximate steady

state solutions for all of the involved quantities. The steady state of the correlation between the structures  $\langle |l_j\rangle \langle u_j| |u_k\rangle \langle l_k| \rangle_{\text{st}}$  is of particular interest. It shows for which parameters the formation of cooperative behavior with the mode is possible [9]. For a given number of structures  $N$  we can calculate the critical temperature  $T_{1,\text{th}}$  that is necessary to meet the condition for cooperative behavior ( $\langle |l_j\rangle \langle u_j| |u_k\rangle \langle l_k| \rangle_{\text{st}} > 0$ ). At the same time, for a given temperature  $T_1$  and the resulting number  $n_2(T_1)$  a certain threshold number  $N_{\text{th}}$  of structures is necessary for cooperative behavior. Details can be found in the supplementary material.

The full set of equations is also integrated numerically to determine the exact steady states and to compare them to the approximate solutions. The parameters  $\kappa = 2\pi \times 5 \times 10^5$  Hz (i.e. FWHM linewidth of 1 MHz),  $g = (\kappa/3) \times 10^{-3}$ ,  $\Delta_u = 0$ ,  $\gamma_1 = 2\pi \times 4 \times 10^2$  Hz,  $\gamma_2 = \gamma_3 = \gamma_4 = \gamma_1 \times 10^2$ ,  $\omega_1 = 2\pi \times 7.9$  THz,  $\omega_2 = 2\pi \times 9$  THz,  $\omega_3 = 2\pi \times 0.1$  THz,  $\omega_4 = 2\pi \times 1$  THz remain fixed for the forthcoming calculations, while  $N$ ,  $T_1$  and  $T_2$  are varied. The number of photons as a function of  $T_1$  and  $T_2$  for  $N = 10^7$  is shown in Fig. 2(a). The occupation of the cavity mode strongly depends on the temperature gradient between the wells. The approximative analytical treatment for small  $T_2$  gives the threshold temperature  $T_{1,\text{th}}$  that signals the onset of cooperative behavior. For  $T_2 > 1$  K the approximative solutions break down. In Fig. 2(b) we show  $\langle a^\dagger a \rangle_{\text{st}}$  as a function of  $T_1$  and  $N$  for fixed  $T_2 = 0.1$  K. Here, the approximative analytical solutions give a reliable result for which parameters to expect a high number of photons in the cavity. The numerical solutions show that the number of photons in the cavity increases rapidly as soon as we exceed  $N_{\text{th}}$  for a given value of  $T_1$ .

Assume that we have a layer containing  $N$  structures which initially is hot. If one side of the layer is cooled by some means, the resulting temperature gradient will lead to a population of the cavity mode. The rate at which photons are lost from the cavity is  $2\kappa \langle a^\dagger a \rangle$ . This suggests that the cavity can serve as a channel for cooling. Without the second quantum well, or equivalently with  $J_1 = J_2 = 0$ , we find the ratio between the upper level  $I_3$  and the lower energy level  $I_2$  in the first well to be  $n_2/(1+n_2)$ . In the presence of the second well, and in the regime where we find a considerable number of photons in the cavity, this ratio is reduced. Figure 3(a) shows how the ratio  $\langle |I_{3,j}\rangle \langle I_{3,j}| \rangle / \langle |I_{2,j}\rangle \langle I_{2,j}| \rangle$  changes with increasing  $T_1$  while  $T_2 = 1$  K remains fixed. With increasing  $T_1$  the relative occupation of the upper level  $|I_{3,j}\rangle$  increases but remains below the result for the uncoupled case. The difference starts to show at  $T_1 \approx 75$  K which is the critical temperature above which we obtain a significant increase in  $\langle a^\dagger a \rangle_{\text{st}}$ , as can be seen in Fig. 2(a). The same comparison can be made for fixed  $T_1 = 400$  K (leaving  $n_2/(1+n_2)$  fixed) and varying  $T_2$ . While  $T_2$  remains low enough to ensure a significant number of

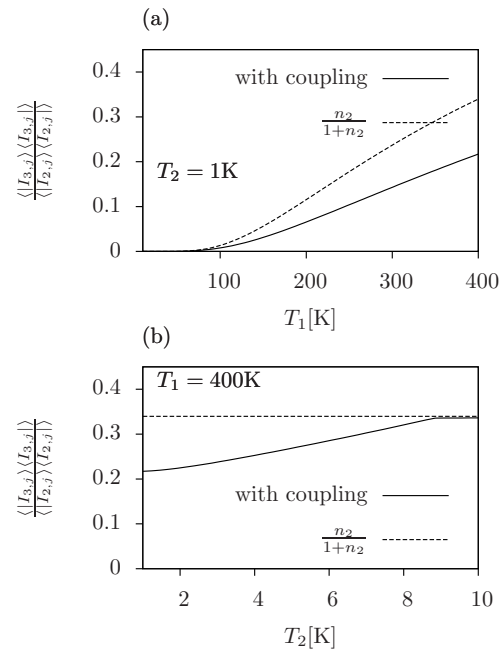


FIG. 3. Occupation ratio in the first quantum well for the coupled and uncoupled case versus  $T_1$  and  $T_2$ . In (a) we choose  $T_2 = 1$  K and vary  $T_1$ . The ratio between the population of  $I_{3,j}$  and  $I_{2,j}$  (solid line) increases with  $T_1$  but remains below the dashed line which gives the ratio in the uncoupled case. In (b) the temperature of the hot part  $T_1$  is fixed to 400 K. For  $T_2 < 9$  K we again see the reduction of  $\langle |I_{3,j}\rangle \langle I_{3,j}| \rangle / \langle |I_{2,j}\rangle \langle I_{2,j}| \rangle$ .

photons in the cavity, and hence a considerable dissipation via the cavity mirrors, the occupation ratio in the first well is reduced. This corresponds to an effectively lower temperature of the first well.

We can obtain a large number of photons in the cavity for  $N > N_{\text{th}}(T_1)$  and an appropriate ratio between  $T_1$  and  $T_2$ . The temperature gradient can therefore be seen as an effective pump. To characterize the emission we calculate the spectrum of the cavity output field and the linewidth. Using the quantum regression theorem we obtain the differential equation for the first order correlation function  $\langle a^\dagger(t+\tau)a(t) \rangle$  and  $\langle |u_j\rangle \langle l_j| (t+\tau)a(t) \rangle$ , see supplementary material. To find the spectrum we calculate the Laplace transform of the coupled equations [10]. The steady state values of the involved quantities are obtained numerically. In Fig. 4 the linewidth (FWHM) of the cavity output spectrum is depicted. With the onset of cooperative behavior the linewidth is reduced dramatically. Similar behavior is found for fixed  $T_2$  and varying  $T_1$  and  $N$ .

The two-well system discussed so far clearly exhibits the essential physical mechanism of heat to coherent light conversion in its purest form. In the following we show that the principle can be extended to multi step excitation processes, where several heat absorbing steps are

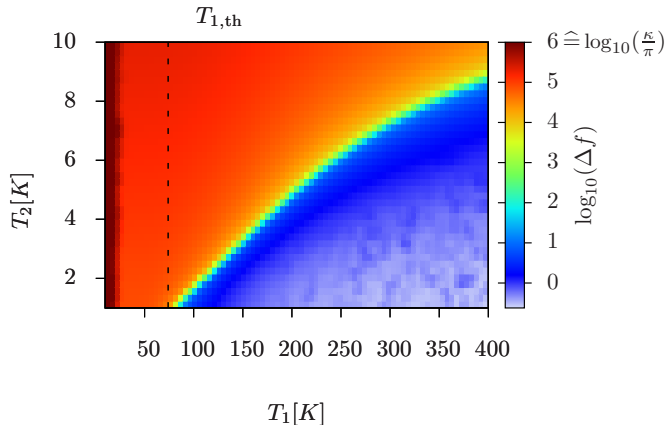


FIG. 4. (Color online) Linewidth of the cavity output spectrum for varying  $T_1$  and  $T_2$  with  $N = 10^7$  (plotted on a logarithmic scale). The linewidth (FWHM) of the empty cavity  $2\frac{\kappa}{2\pi} = 1$  MHz corresponds to the dark red color (upper boundary of the scale). The linewidth  $\Delta f$  falls slightly below that limit with increasing  $T_1$  until it finally drops off dramatically as the cooperative effects emerge. For small  $T_2$  the onset of cooperative behavior is marked by  $T_{1,\text{th}}$ .

combined to lead to operation at higher emission frequencies. Mathematically, this can be easily facilitated by incorporating an absorptive step in the second well by choosing  $\omega'_u > \omega_4$ , without needing a more complex model. In the dissipative dynamics we simply have to exchange the rates  $\gamma_3 n_3(T_2) \leftrightarrow \gamma_3 (n_3(T_2) + 1)$ . Physically, this means that in each cycle in this system the absorption of an extra thermal photon or phonon with frequency  $\omega'_u - \omega_{I_4}$  is necessary. This implies that we find a minimal temperature below which not enough phonons are present and lasing is impossible. In general one could of course even think of a combination of thermally assisted and externally driven excitation steps. We will refrain from this here to keep the complexity of the model limited.

Let us look at the results now. The temperature range for which  $\langle a^\dagger a \rangle_{\text{st}}$  becomes significant is depicted in Fig. 5(a). The dashed line marks the critical temperature necessary for cooperative behavior, which is obtained analytically with similar approximations as described above. The linewidth of the emission is shown in Fig. 5(b). This concept could be incorporated as an extra step in conventional quantum well lasers, which generate intrinsic heat during operation, to extend their range of operation as the absorption of phonons would counteract the heating process.

Our theoretical calculations exhibit the possibility to use a spatial temperature gradient in a suitable active medium to induce optical gain and lasing. While not very practicable in the visible regime, a semiconductor heterostructure can be envisaged to generate narrow band-

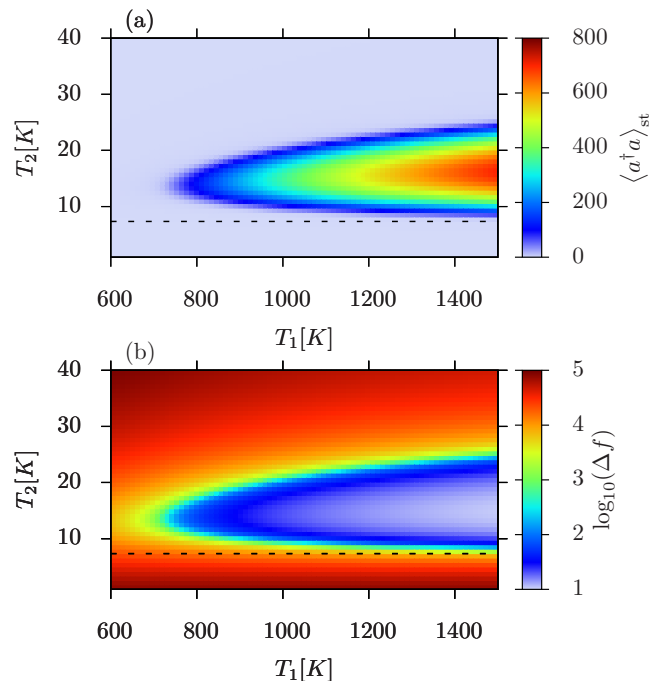


FIG. 5. (Color online) (a) Number of photons in the mode versus  $T_1$  and  $T_2$ . For  $T_2 > T_{2,\text{th}}$  we find a sudden increase in  $\langle a^\dagger a \rangle_{\text{st}}$ , and in (b) a corresponding drop in the linewidth of the cavity emission. The parameters remain unchanged except for  $\gamma_3 = \gamma_1 = 2\pi \times 4 \times 10^2$  and  $\omega'_u = \omega_u + 2\pi \times 0.2$  THz.

width emission through a resonant cavity mode in the THz regime, where the coherent emission of photons is sustained by the spatial temperature gradient. The effective extraction of thermal energy from the system in parallel provides for stimulated cooling of the first, hot quantum well. To use a similar idea at higher frequencies without too high temperatures, a multi step excitation process can be envisaged, where some steps could also invoke optical pumping or current injection. In general, introducing an absorptive step well before carrier injection to the upper laser level relies on absorption of thermal quanta and therefore counteracts heating during operation. This leads to a higher operating temperature limit. While we here only worked with an oversimplified generic model, the physical principles behind should stay valid for more realistic and thus more complex descriptions. In addition, transverse spatial temperature gradients or even spatially separated structures connected by conducting wires might provide for alternative configurations at greater length scales.

K.S. was supported by the DOC-fORTE doctoral program of the ÖAW. H.R. acknowledges support from the Austrian Science Fund FWF grant S4013.

- 
- [1] W. Lamb Jr, Phys. Rev **134**, A1429 (1964).  
 [2] E. Boukobza and D. Tannor, Physical Review A **74**, 063822 (2006).  
 [3] M. Youssef, G. Mahler, and A. Obada, Physica E: Low-dimensional Systems and Nanostructures **42**, 454 (2010).  
 [4] R. Graham and H. Haken, Zeitschrift für Physik A Hadrons and Nuclei **237**, 31 (1970).  
 [5] S. Kumar, C. Chan, Q. Hu, and J. Reno, Nature Physics **7**, 166 (2010).  
 [6] R. Epstein, M. Buchwald, B. Edwards, T. Gosnell, and C. Mungan, Nature **377**, 500 (1995).  
 [7] H. Carmichael, *An open systems approach to quantum optics: lectures presented at the Université libre de Bruxelles, October 28 to November 4, 1991*, Vol. 18 (Springer,

1993).

- [8] R. Kubo, Journal of the Physical Society of Japan **17**, 1100 (1962).  
 [9] D. Meiser, J. Ye, D. Carlson, and M. Holland, Physical review letters **102**, 163601 (2009).  
 [10] P. Meystre and M. Sargent, *Elements of quantum optics* (Springer Verlag, 2007).

## SUPPLEMENTARY MATERIAL

### Liouvillian

The Liouvillian that describes dissipative processes, including the coupling of the cavity and the structures to the environment at finite temperature, reads

$$\begin{aligned}
 \mathcal{L}[\rho] = & \kappa (n_1 (T_2) + 1) (2a\rho a^\dagger - a^\dagger a\rho - \rho a^\dagger a) + \kappa n_1 (T_2) (2a^\dagger \rho a - aa^\dagger \rho - \rho aa^\dagger) \\
 & + \gamma_1 (n_1 (T_2) + 1) \sum_j (2|l_j\rangle \langle u_j| \rho |u_j\rangle \langle l_j| - |u_j\rangle \langle u_j| \rho - \rho |u_j\rangle \langle u_j|) \\
 & + \gamma_1 (n_1 (T_2)) \sum_j (2|u_j\rangle \langle l_j| \rho |l_j\rangle \langle u_j| - |l_j\rangle \langle l_j| \rho - \rho |l_j\rangle \langle l_j|) \\
 & + \gamma_2 (n_2 (T_1) + 1) \sum_j (2|I_{2,j}\rangle \langle I_{3,j}| \rho |I_{3,j}\rangle \langle I_{2,j}| - |I_{3,j}\rangle \langle I_{3,j}| \rho - \rho |I_{3,j}\rangle \langle I_{3,j}|) \\
 & + \gamma_2 (n_2 (T_1)) \sum_j (2|I_{3,j}\rangle \langle I_{2,j}| \rho |I_{2,j}\rangle \langle I_{3,j}| - |I_{2,j}\rangle \langle I_{2,j}| \rho - \rho |I_{2,j}\rangle \langle I_{2,j}|) \\
 & + \gamma_3 (n_3 (T_2) + 1) \sum_j (2|u_j\rangle \langle I_{4,j}| \rho |I_{4,j}\rangle \langle u_j| - |I_{4,j}\rangle \langle I_{4,j}| \rho - \rho |I_{4,j}\rangle \langle I_{4,j}|) \\
 & + \gamma_3 (n_3 (T_2) (T_2)) \sum_j (2|I_{4,j}\rangle \langle u_j| \rho |u_j\rangle \langle I_{4,j}| - |u_j\rangle \langle u_j| \rho - \rho |u_j\rangle \langle u_j|) \\
 & + \gamma_4 (n_4 (T_2) + 1) \sum_j (2|I_{1,j}\rangle \langle l_j| \rho |l_j\rangle \langle I_{1,j}| - |l_j\rangle \langle l_j| \rho - \rho |l_j\rangle \langle l_j|) \\
 & + \gamma_4 (n_4 (T_2)) \sum_j (2|l_j\rangle \langle I_{1,j}| \rho |I_{1,j}\rangle \langle l_j| - |I_{1,j}\rangle \langle I_{1,j}| \rho - \rho |I_{1,j}\rangle \langle I_{1,j}|) \quad . \quad (8)
 \end{aligned}$$

---

### Approximate Analytical Solutions

For  $T_2$  small enough we can neglect  $n_1$ ,  $n_3$  and  $n_4$ . Inserting the steadystate solutions for  $\langle a | u_j \rangle \langle l_j | \rangle_{\text{st}}$ ,  $\langle | u_j \rangle \langle u_j | \rangle_{\text{st}}$  and  $\langle | l_j \rangle \langle l_j | \rangle_{\text{st}}$  into Eq. (6) we obtain

$$\begin{aligned}
& 2 \langle |l_j\rangle \langle u_j | u_k \rangle \langle l_k | \rangle_{\text{st}} \left[ \gamma_1 + \gamma_4 \right. \\
& + \left( g^4 N^2 |J_2|^2 \langle |l_j\rangle \langle u_j | u_k \rangle \langle l_k | \rangle_{\text{st}} (2 + 3n_2) \gamma_2 \gamma_3 (\gamma_2 + n_2 \gamma_2 + \gamma_3) \gamma_4 + |J_1|^2 \left( g^4 N^2 \langle |l_j\rangle \langle u_j | u_k \rangle \langle l_k | \rangle_{\text{st}} n_2^2 \gamma_2^2 \gamma_3 \gamma_4 \right. \right. \\
& \left. \left. + |J_2|^2 (2g^4 N^2 \langle |l_j\rangle \langle u_j | u_k \rangle \langle l_k | \rangle_{\text{st}} ((\gamma_2 + \gamma_3) \gamma_4 + n_2 \gamma_2 (\gamma_3 + 2\gamma_4)) + g^2 N n_2 \gamma_2 \gamma_3 (\gamma_1 - \gamma_4) \kappa + n_2 \gamma_2 \gamma_3 (\gamma_4^2 - \gamma_1^2) \kappa^2) \right) \right) \\
& \left. / \left( \gamma_1 \kappa^2 \left( |J_2|^2 (2 + 3n_2) \gamma_2 \gamma_3 (\gamma_2 + n_2 \gamma_2 + \gamma_3) \gamma_4 + |J_1|^2 (n_2^2 \gamma_2^2 \gamma_3 \gamma_4 + 2 |J_2|^2 ((\gamma_2 + \gamma_3) \gamma_4 + n_2 \gamma_2 (\gamma_3 + 2\gamma_4))) \right) \right) \right) \right] = 0
\end{aligned} \tag{9}$$

for the quantity  $\langle |l_j\rangle \langle u_j | u_k \rangle \langle l_k | \rangle_{\text{st}}$  describing cooperative behavior between the structures. The stable solution is obtained from the part of Eq. (9) which is en-

closed by the rectangular brackets. To find the number of structures necessary for reaching the onset of cooperative behavior  $N_{\text{th}}(T_1)$  for a given temperature  $T_1$  we solve  $\langle |l_j\rangle \langle u_j | u_k \rangle \langle l_k | \rangle_{\text{st}} = 0$  to find

$$\begin{aligned}
N_{\text{th}}(T_1) = & \left( (\gamma_1 + \gamma_4) \kappa \left( |J_2|^2 (2 + 3n_2) \gamma_1 \gamma_2 \gamma_3 (\gamma_2 + n_2 \gamma_2 + \gamma_3) \gamma_4 \right. \right. \\
& \left. \left. + |J_1|^2 (n_2^2 \gamma_1 \gamma_2^2 \gamma_3 \gamma_4 + |J_2|^2 (2\gamma_1 (\gamma_2 + \gamma_3) \gamma_4 + n_2 \gamma_2 (\gamma_1 \gamma_3 + 4\gamma_1 \gamma_4 + \gamma_3 \gamma_4))) \right) \right) \\
& / \left( g^2 n_2 \gamma_2 \gamma_3 (\gamma_4 - \gamma_1) |J_1|^2 |J_2|^2 \right). \tag{10}
\end{aligned}$$

The result is plotted in Fig. 2(b) (dashed line). Similar calculations give the critical temperature  $T_{1,\text{th}}$  for given  $N$ , see Fig. 2(a).

### Calculation of the spectrum

Using the quantum regression theorem we obtain  $\langle a^\dagger(t + \tau) a(t) \rangle$  which couples to  $\langle |u_j\rangle \langle l_j | (t + \tau) a(t) \rangle$ . For  $t \rightarrow \infty$  using stationarity we can write

$$\frac{d}{d\tau} \left( \langle a^\dagger(\tau) a(0) \rangle \right) = \begin{pmatrix} -\kappa & -igN \\ -ig \langle |u_j\rangle \langle u_j | \rangle_{\text{st}} & i\Delta_u - \Gamma \end{pmatrix} \times \begin{pmatrix} \langle a^\dagger(\tau) a(0) \rangle \\ \langle |u_j\rangle \langle l_j | (\tau) a(0) \rangle \end{pmatrix} \tag{11}$$

with  $\Gamma = \gamma_3 n_3 (T_2) + \gamma_1 (2n_1 (T_2) + 1) + \gamma_4 (n_4 (T_2) + 1)$ . The Laplace transformation yields

which allows to calculate the spectrum [10].

$$\langle a^\dagger a \rangle(s) = \frac{\langle a^\dagger a \rangle_{\text{st}} (s - i\Delta_u + \Gamma) - igN \langle |u_j\rangle \langle l_j | a \rangle_{\text{st}}}{(s + \kappa) (s - i\Delta_u + \Gamma) - g^2 N (\langle |u_j\rangle \langle u_j | \rangle_{\text{st}} - \langle |l_j\rangle \langle l_j | \rangle_{\text{st}})} \tag{12}$$